This article has been accepted for publication. Content may change prior to final publication.
Citation information: DOI 10.1109/JPHOTOV.2016.2581481 IEEE Journal of Photovoltaics

Optimized Configuration of Mismatched Photovoltaic Arrays

M.L. Orozco-Gutierrez, G. Spagnuolo, J.M. Ramirez-Scarpetta, G. Petrone, and C.A. Ramos-Paja

***Abstract*—When the panels in a photovoltaic (PV) array are subjected to a non uniform irradiance level, some bypass diodes may turn on and the overall power production might be affected significantly. An increase of the power delivered by the whole array might be obtained by means of its electrical reconfiguration, that is the change of the series-parallel connection among the panels it is made up of. The computation of the electrical connection among the panels that ensures the maximum delivered power is a combinatorial problem requiring powerful optimization methods. This paper is devoted to the formulation of an optimization procedure for determining the best electrical configuration among the panels. The proposed algorithm requires simple mathematical calculations, and it uses a vectorized structure, thus it is suitable to be implemented in any embedded system for the purpose of a real-time PV array reconfiguration. The algorithm is firstly explained by using a pilot example and afterwards its performance is shown by applying it to a real domestic photovoltaic field. The results show that the optimization algorithm computes an optimized configuration with a low computational burden.**

***Index Terms*—Photovoltaic Systems, Reconfiguration, Optimization, Constraints.**

NOMENCLATURE

G	Irradiance level.
$I_{higher}(Qm^{'})$	Number of modules able to work at higher MPP current candidate.
$I_{lower}(Qm^{'})$	Number of modules able to work at lower MPP current candidate.
I_{mpp}	MPP current.
I_{sc}	Short circuit current.
k	Index to identify a MPP in a string.
M	Number of modules in a panel.
m	Index to identify a MPP of a module.
M_a	Number of active modules.
M_{na}	Number of non-active modules.
n	Index to identify a MPP in an array.
$N_{I_{mpp}}$	Number of MPP current candidates.
$n_{p,st}$	Number of panels in a string.
N_p	Number of panels in the PV field.
Qm	Number of modules able to work at a MPP current candidate.
V_d	Voltage forward drop of a bypass diode.
$V_{inv_{max}}$	Maximum input voltage of an inverter.
$V_{inv_{min}}$	Minimum input voltage of an inverter.
V_{mpp}	MPP voltage.
V_{oc}	Open circuit voltage.

M.L. Orozco-Gutierrez and J.M. Ramirez-Scarpetta are with Universidad del Valle, Colombia e-mail: (martha.orozco@correounivalle.edu.co, jose.ramirez@correounivalle.edu.co).

G.Spagnuolo and G. Petrone are with University of Salerno, Italy e-mail: (gspagnuolo@unisa.it, gpetrone@unisa.it).

C.A. Ramos-Paja is with Universidad Nacional de Colombia, Colombia e-mail: (caramosp@unal.edu.co).

I. INTRODUCTION

Photovoltaic (PV) plants operating in non-uniform conditions may exhibit a Power vs. Voltage (P-V) curve with multiple local Maximum Power Points (MPPs) [1], which are generated by the turning on of some bypass diodes. Module dedicated electronics might be helpful in reducing the power drop that is a consequence of the mismatched conditions, but the change of the electrical connection among the panels is a recent appealing solution [2],[3]. In the scientific literature, the reconfiguration applications use different hardware structures, where the most common architectures are series-parallel (SP) and Total-Cross-Tied (TCT) [3]. The problem to determine the optimal solution of the connection among PV panels has been addressed from different approaches, being irradiance equalization and sorting algorithms the most reported ones [3]. In a possible implementation of PV reconfiguration system [2], periodically during the day, a switching matrix connects a suitable switching converter to each PV panel, after having disconnected it from the PV field, for acquiring its Current vs. Voltage (I-V) curve. Afterwards, a processing unit uses these curves to determine the new connection among the panels that ensures the maximum PV field overall power. Finally, the same switching matrix settles the new PV field topology just determined. This procedure enables to detect the presence, in more than one string, of panels receiving a high irradiance level and of others receiving a lower one. The reconfiguration algorithm likely reorganizes the two strings by collecting the former panels in series in one string and the latter ones in the second string, so that the bottleneck effect is decreased [2], the number of active bypass diodes is minimized and the overall power production is increased. However, in sparse mismatching conditions the distribution of panels among highly and lowly irradiated is not inmediate. For these cases, an increase of the number of strings in the array and an exhaustive search to determine the configuration, as is presented in [4], can be a solution. However, another compromise between cost, efficiency and number of strings appears, it because a converter with non-unitary efficient have to be connected in each string. Moreover, exhaustive methods can be adopted for practical reconfiguration systems involving a small number of PV panels. Unfortunately, in medium and large PV systems the number of combinations is prohibitive and algorithms based on linear programming, recursion and

enumeration, heuristics, statistical sampling methods, among others, can be used, but at the price of not being sure that the global optimal solution is achieved [5].

The complexity of the reconfiguration problem is increased due to the fact that some or even all the panels in the field can be subjected to partial shading, so that the P-V curve of each panel shows more that one MPP. Moreover, the panels, and not modules, reconfiguration process has to be realized, so that modules providing the highest power could be grouped separately [6],[7],[4]. In the same way, a reconfiguration of mismatched panels based on a minimization of irradiance levels of rows in a TCT configuration is not direct, as the case of modules [8].

In literature, a first approach to this optimization problem using genetic algorithms was presented in [9]. However, the computational burden is significant and the algorithm is not able to guarantee the detection of the best configuration.

This paper proposes an optimization algorithm for reconfiguring PV arrays, which uses an approach that selects a configuration providing the higher power value into a set of MPP candidates. The proposed algorithm uses a very short computation time, and it only requires to know the voltage and current values of all the MPPs of every PV panel, such as it will be explained in section two. The optimization algorithm is organized in two main steps. The first one allows to identify the voltage and current values where the MPP candidates of the PV array might occur, which will be detailed in sections three and six for string and array configurations, respectively. The second step consists in the construction of a matrix including all the MPPs associated to a number of configurations of the PV array. In section fourth will be demonstrated that the position of the maximum values in that matrix gives a direct information of which panels must be included in the same string. An estimation of the MPPs coordinates (V_{mpp}, I_{mpp}), which has been done for reducing the computation time, does not affect the identification of the optimized configuration. The steps of the proposed optimization algorithm are explained through some small examples. In section seven, a practical example is used to compare the results of the proposed method with the results obtained by performing the exhaustive search. Finally, conclusion are given.

II. Assumptions

In this paper the following definitions of array, string, module and panel are used. A PV array is formed by the parallel connection of PV strings, which are in turn the series connection of PV panels. A typical PV panel consists of the series connection of two or three PV modules, which are the series connection of PV cells with an anti-parallel bypass diode. A graphical representation of those definitions is given in the figure 1.

The approach proposed in this paper is based on the following assumptions.

First, it is assumed that the current vs. voltage (I-V) curve of each Photovoltaic (PV) panel is acquired and processed by means of the algorithm presented in [10]. That algorithm analyzes the samples of the panel I-V curve by discovering the

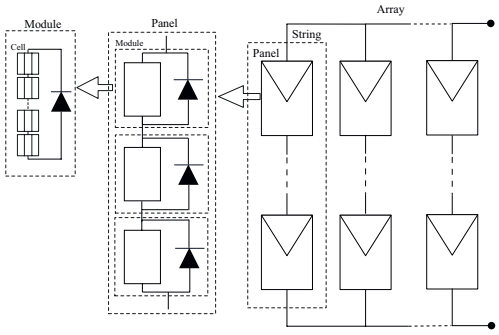

Figure 1. Definition of PV Array, String, Panel and Module

constant-current and the constant-voltage regions, thus recognizing the coordinates of the maximum and minimum power points of the corresponding P-V curve, in a computationally efficient way. In figure 2 an example of these data, for a PV panel subjected to uniform and mismatching conditions, is presented. In this example, the maximum and minimum power points, provided by [10], are highlighted in green and yellow markers. Moreover, algorithm [10] provides the short circuit current and the open circuit voltage, which are marked in black and magenta colors, respectively.

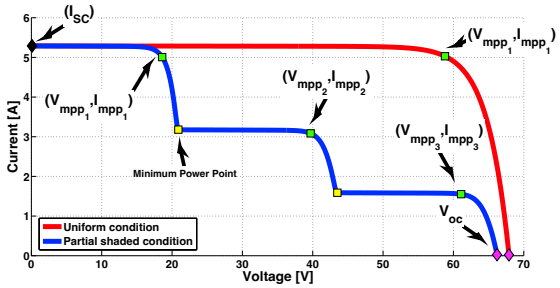

Figure 2. Data set provided by [10] for a PV panel subjected to uniform and mismatching conditions

It is also assumed that all the panels in the PV field (N_p) are made of the same number (M) of modules. The index m is used to identify the MPP voltage and current of a particular module, which are (V_{mpp_m}, I_{mpp_m}). These coordinates are obtained by the direct estimation proposed in [11], in which the data provided by [10] and the voltage of the conducting bypass diodes, are used.

Moreover, it is assumed that the strings of the PV array have the same number of panels $n_{p,st}$ connected in series. In other words, the parallel connected strings are assumed to have the same length. This choice is motivated by the fact that uneven strings connected in parallel can cause current back flows in the shorter string [2].

III. The optimization algorithm

In the flow chart of Fig.3, the general steps of the optimization algorithm are presented. In the first step, by using the algorithms [10],[11], the I_{mpp} and V_{mpp} of all the modules are calculated. After, the voltage and current intervals for the

string MPPs are calculated. Next, by multiplying those voltage and current candidates, the candidates MPPs for any configuration of the panels are determined. A matrix representation of the MPP candidates is introduced to determine the string configurations providing the absolute MPP. This matrix also to keep into account the voltage constraints imposed by the inverter. The proposed optimization algorithm is explained by using a pilot example, so a more detailed description of the steps presented in Fig.3 will be provided in section V. The extension of the method to a PV field including multiple strings connected in parallel will be given in Section VI.

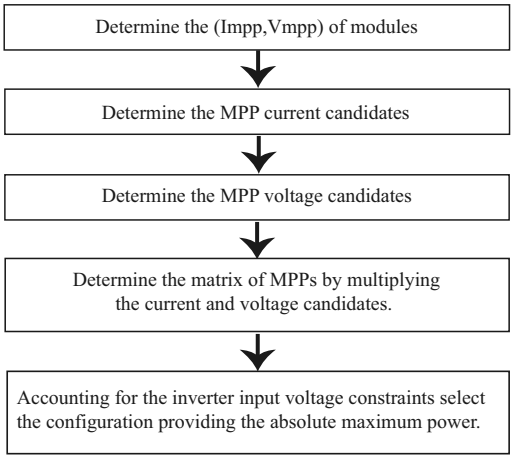

Figure 3. Flow chart of the optimization algorithm

The pilot example refers to a string of three PV panels (P1,P2,P3), thus $N_p = 3$, each one made of three PV modules, thus $M = 3$. Then, given the I-V curve of each panel, the procedures [10],[11] provide the data of the modules (V_{mpp_m}, I_{mpp_m}) presented in table I. Moreover, the additional information concerning the irradiance level G_m and MPP power MPP_m of each module have been added for illustrative purposes. All the three panels have three MPPs because it is assumed that all the modules work in different conditions. The objective is to obtain the maximum possible power by using all the three panels or only a subset of them.

Table I
DATA SET OF THE PV PANELS IN THE PILOT EXAMPLE

Panels	V_{mpp_m} [V]	I_{mpp_m} [A]	MPP_m [W]	G_m $[W/m^2]$
P1	[19.5, 19.2, 17.7]	[4.5, 2.6, 1.6]	[87.8, 49.9, 28.3]	[900, 500, 300]
P2	[19, 18.6, 16.5]	[2.5, 1.5, 0.5]	[47.5, 27.9, 8.3]	[500, 300, 100]
P3	[19.4, 19.4, 18]	[4.0 3.1 2.1]	[77.6, 60.1, 37.8]	[800, 600, 400]

If one, two or even three of those panels are connected in series, the evaluation of the resulting string MPPs is not straightforward. The MPPs voltage and current coordinates are evaluated through a procedure, illustrated below, which is based on the validation of a number of candidate solutions.

A. String MPP current candidates

As previously demonstrated in [12] and formalized in (1), the candidates string MPP currents I_{mpp_k} are very close to the corresponding MPP currents at module level I_{mpp_m}:

$$I_{mpp_k} \simeq I_{mpp_m} \qquad \forall k \in \{1, 2, ..., K\} \qquad \forall m \in \{1, 2, ..., M\} \tag{1}$$

According to the assumptions given in the previous section, the MPPs of the modules are known, thus using (1) the MPP current candidates of the string are calculated. For the pilot example, the MPPs of the modules are given in table I. The amount of I_{mpp_k} candidates can be reduced depending on the irradiance profile. Indeed, PV modules subjected to the same irradiance level give rise to the same I_{mpp_k} candidate. Moreover, in order to filter out inaccuracies and noise of the measurement process, in this work the I_{mpp_m} values differing by less than 5% are assumed to be equal, thus a further reduction in the number of candidate MPP currents is achieved. In the pilot example, the I_{mpp_k} candidates, sorted in ascending order, are: $I_{mpp_k} = [0.5, 1.5, 1.6, 2.0, 2.5, 2.6, 3.1, 4.0, 4.5]$. The candidates $I_{mpp_2} \cong I_{mpp_3}$ and $I_{mpp_5} \cong I_{mpp_6}$, thus, the final MPPs candidates are given by the vector in (2), where $N_{I_{mpp}} = 7$ is the length of this vector.

$$I_{mpp_k} = [0.5, 1.5_{(2)}, 2.0, 2.5_{(2)}, 3.1, 4.0, 4.5] \pm 5\% \tag{2}$$

In the parentheses the multiplicity of some candidates has been put into evidence, thus the information concerning PV modules having the same I_{mpp} current is preserved. When not explicitly evidenced, the multiplicity of the candidate is equal to one. Thus, for the pilot example, the second and fourth value in this vector have multiplicity equal to 2.

B. String MPP voltage candidates

The prediction of the string MPPs voltage coordinates V_{mpp_k} is not straightforward as for the currents. Indeed, for each string MPP current I_{mpp_k}, all the modules having their short circuit current I_{sc_m} lower than I_{mpp_k} are bypassed. Thus those modules show a negative voltage, which is the voltage forward drop V_d of their own bypass diode. Figure 4 shows an example of the construction of a PV string I-V curve (right side plot) from the I-V curves (left side plot) of the six modules that are included in two panels. The MPPs of the string and of each module are highlighted in green color. For instance, the string MPP marked with "A" in figure 4 is obtained by having the modules M1, M2 and M3, with a MPP current higher than the one of point "A", i.e. working on the right side of their MPPs, thus in the voltage ranges $[V_{mpp_m}, V_{oc_m}]$, m=1,2,3. Instead, modules M5 and M6, having MPP currents that are lower than the current in "A", work at a negative voltage value imposed by their own bypass diodes that are active at the "A" MPP. The only module working close to its own MPP is M4.

Usually, PV modules exhibit MPP voltages V_{mpp_m} that are within $[73 - 80]\%$ of the open circuit voltage V_{oc_m} [13], [14], [15]. Therefore, the operating voltage of active modules falls in the range $[V_{mpp_m}, 1.37 \cdot V_{mpp_m}]$, because for every module working on the right side of its MPP the maximum value of the open circuit voltage is $V_{oc_m} \cong (1/0.73) \cdot V_{mpp_m} = 1.37 \cdot V_{mpp_m}$. By referring to the MPP "A" in figure 4, the voltage contribution from the active modules $(M1, M2, M3, M4)$ is within the interval $[\sum_{i=1}^{4} V_{mpp_i}, 1.37 \cdot (\sum_{i=1}^{4} V_{mpp_i})]$. The

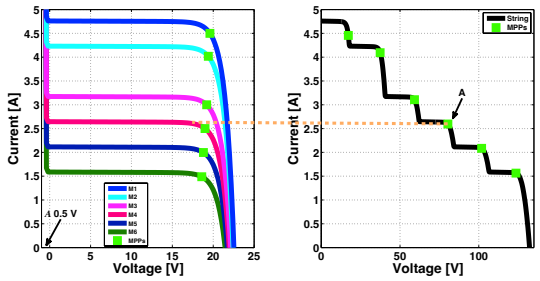

Figure 4. Relationship between the MPPs of a string and the MPPs of its modules

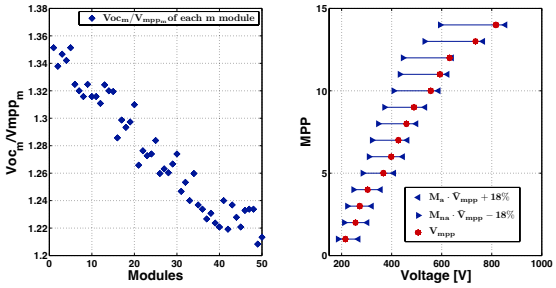

Figure 5. V_{mpp} of a string falling into the approximated range $[M_a \cdot \bar{V}_{mpp}] \pm 18\%$

upper bound of this interval is overestimated because it is calculated by adding the open circuit voltage of each module. Thus, it is reasonable to approximate the maximum string voltage by averaging the V_{mpp} and V_{oc} values, i.e. $1.18 \cdot V_{mpp_m}$ instead of $1.37 \cdot V_{mpp_m}$. This approximation compensates the overestimated operating voltages of some modules with the underestimated operating voltages of other ones.

Moreover, although V_{mpp_m} is different for each module due to the mismatched working conditions, usually the difference among the V_{mpp_m} values is small. Hence the mean value $\bar{V}_{mpp}$ of all the modules is used to estimate the MPPs voltages in the string. Therefore, the voltage contribution from the active modules at the point "A" is within the interval $[M_a \cdot \bar{V}_{mpp}, 1.18 \cdot M_a \cdot \bar{V}_{mpp}]$, where M_a is the number of active modules in the string.

On the other hand, the negative voltage contribution from the non-active modules $(M5, M6)$ at the MPP "A" is obtained multiplying the number of non-active modules (M_{na}) by the average voltage of the bypass diodes $(V_d \approx 0.5V)$. Thus the positive and negative voltage contributions are combined and the final voltage interval in which the string MPP voltage "A" falls is given by: $[(M_a \cdot \bar{V}_{mpp} - M_{na} \cdot V_d), 1.18 \cdot M_a \cdot \bar{V}_{mpp}]$. In the real cases, the number of non-active modules is lower than the active ones $(M_{na} < M_a)$. Moreover, the voltage drop V_d is lower than $0.18 \cdot V_{mpp}$, thus the previous interval is always included in the range $[M_a \cdot \bar{V}_{mpp}] \pm 18\%$. The latter can be calculated straightforwardly because it depends on to the number of active modules only.

The accuracy of the proposed approximation has been tested by analyzing a string of 50 PV modules subjected to a sparse irradiance profile. Moreover, parametric variations of 5% among the modules have been also introduced. The calculation of the fraction V_{oc_m}/V_{mpp_m} is presented on the left side of figure 5. It is observed that the characteristic of the modules involves the best and the poor cases of V_{oc_m}/V_{mpp_m}, which are close to the values $\frac{1}{0.8} \approx 1.25$ and $\frac{1}{0.73} \approx 1.37$ respectively. In this example the PV string exhibits 14 MPPs, and their V_{mpp} fall within the approximated interval of voltage $[M_a \cdot \bar{V}_{mpp}] \pm 18\%$, such is shown on the right side of figure 5. By using those previous considerations in the pilot example, the mean value of the MPP voltages listed in table I is $19.3V$, and the vector of the string MPP voltage candidates is given in (3), which includes the tolerance 18% previously discussed.

$$V_{mpp_k} = [19.3, 38.6, 57.9, 77.2, 96.5, 115.8, 135.1, 154.4, 173.7] \pm 18\% \quad (3)$$

C. MPP candidates

Once given the coordinates of the possible MPPs, in voltage by (3) and in current by (2), it is possible to define an effective procedure to find the connections ensuring the maximum absolute power production, which is the main contribution of this work. Otherwise, a time consuming exhaustive search would have to be used.

The first step is the assessment of the MPP candidates. A candidate string is able to generate power at a specific couple (V,I) depending on the number of modules that are able to work at the given current. For example, by considering the current value $4.0A$, the data set values (2) reveal that only two modules exhibit MPP currents higher than or equal to $4.0A$. Thus a string formed by these two modules can operate at $4.0A$ at a voltage value not higher than $38.6 \pm 18\%$. The latter is the maximum voltage at which two modules in series connection can work as given in (3). In conclusion, by referring to the pilot example, for having a string working at $4.0A$ no more than the two mentioned modules, thus no more than the two PV panels including them, can be taken. In that case, The MPP power is $4.0 \times 38.6 = 154.4W$. This reasoning can be done for every value of the vector (2). For instance, at $0.5A$ all the modules are able to work, thus there are as many MPPs as the number of voltage candidates given in the vector (3). Again, at $1.5A$, that is the second value in (2), can work eight modules operating at least at $1.5A$. Instead, at $2.0A$ only six modules can be included in the string, because of the multiplicity equal to 2 of the module at $1.5A$. Finally, a vector is constructed to store the number of modules that can be included in the string for each MPP current candidate. As for the pilot example, this vector is given in (4):

$$Qm_k = [9, 8, 6, 5, 3, 2, 1] \quad (4)$$

In this pilot example, $Qm_4 = 5$ means that there are five modules able to generate power at the MPP current candidate I_{mpp_4}, which is $2.5A$. In the same way, five modules in series connection provide a maximum voltage close to the fifth element of the vector reporting the MPP voltage candidates, which is $96.5 \pm 18\%V$. Finally, a matrix representation of the MPP candidates is obtained as it is given in (5). For each MPP current (2) and voltage (3) candidate, their product is calculated. After, these products fill the matrix (5), but the products representing unfeasible MPPs are replaced by

a zero. It is worth noting that the number of elements to be zeroed at the bottom of each column of the matrix (5) can be determined immediately by looking at the vector (4). Indeed, the numbers collected in the vector (4) and representing the maximum number of modules working at a given I_{mpp} string current, correspond to the numbers of non-zero elements in each column of matrix (5). For example: the first column of (5), corresponding to $0.5A$, has nine non-zero elements; the second one, corresponding to $1.5A$, has eight non-zero elements and so on.

$$\begin{array}{c|c} \frac{I\Rightarrow}{V\Downarrow} & |0.5 \quad 1.5 \quad 2.1 \quad 2.5 \quad 3.1 \quad 4.0 \quad 4.5| \\ \hline 19.3 & \begin{pmatrix} 9.8 & 29.7 & 40.00 & 48.2 & 59.5 & 77.5 & 87 \\ 38.6 & 19.68 & 59.29 & 79.89 & 96.39 & 118.99 & 154.92 & 0 \\ 57.9 & 29.52 & 88.94 & 119.84 & 144.59 & 178.48 & 0 & 0 \\ 77.2 & 39.36 & 118.59 & 159.79 & \mathbf{192.79} & 0 & 0 & 0 \\ 96.5 & 49.20 & 148.24 & \mathbf{199.74} & \underline{\mathbf{241.0}} & 0 & 0 & 0 \\ 115.8 & 59.04 & 177.88 & \mathbf{239.68} & 0 & 0 & 0 & 0 \\ 135.1 & 68.88 & \mathbf{207.53} & 0 & 0 & 0 & 0 & 0 \\ 154.4 & 78.72 & \mathbf{237.18} & 0 & 0 & 0 & 0 & 0 \\ 173.7 & 88.56 & 0 & 0 & 0 & 0 & 0 & 0 \end{pmatrix} \end{array} \quad (5)$$

IV. Selection of the best configuration

Matrix (5) contains all feasible MPP candidates. The absolute maximum is ensured by putting five modules in series working at $2.5A$: indeed, the element of coordinates (5,4) shows the maximum value. Thus, table I reveals that the five modules having a current higher than $2.5A$ must be taken and the PV panels they belong to must be connected in series. This is the best string ensuring the maximum absolute power. Although, this examination can be performed easily by any searching algorithm, the flow chart shown in figure 6 explains the mechanism. On the right side of this flow chart, the results provided by each step, for the pilot example, are shown. In the first step, the modules that are able to work at the MPP current candidate $(2.5A)$ are selected. It is evident that the panels P1 and P3 have two modules working at a current higher than $2.5A$ while the panel P2 has only one. In the second step, such calculation is done. Afterwards, the panels are sorted with a decreasing number of modules that are able to work at that MPP current, so that the voltage candidates are selected. Finally, all the three panels are connected in series to ensure the MPP candidate delivers $241.0W$.

However, it is worth noting that two elements must be taked into account to select the global MPP: the tolerance among the MPP candidates and the fact that the input voltage of the inverter has to fall within a given interval.

A. Accounting for the tolerance of MPP candidates

Due to the tolerances introduced in (3) for the voltages, which also affect the current candidates (2), a $\pm 23\%$ tolerance on the MPP power must be kept into account. This means that some other candidates that might be comparable with the one already mentioned are in the power range $241.0W - 23\% = [185.57, 241.00]W$. Thus the corresponding string configurations should be analyzed before deciding which is the best one. By looking at (5), it is evident that the solutions including six and five modules working at $2.1A$ must be also accounted for since they provide $239.7W$ and $199.74W$, respectively. Moreover, the solutions with eight and seven modules working at $1.5A$ are also candidates, which provide $237.2W$ and $207.5W$, respectively. These other MPP candidates have been bolded in (5). Moreover, the position of the best value in the power matrix gives searching criteria for the optimized configuration: the row provides the number of modules to search, so that number of modules are able to work at the current level, given by the column index, providing positive voltage. It is worth noting that, in general, even if this case does not occur in the pilot example, more than one configuration can give the same power candidate. In that case some further design constraint, such as the inverter input voltage requirement, might be useful to choose the best one.

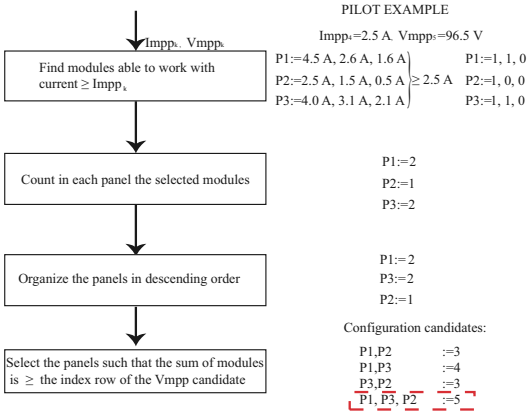

Figure 6. Flow chart of the searching algorithm of the candidate configurations

B. Accounting for the inverter input voltage constraints

A commercial inverter taking the PV string at its DC input is able to perform the MPPT function in a voltage range $[V_{inv_{min}}, V_{inv_{max}}]$, this meaning that the MPP must fall within this range. In order to comply with this constraint, some rows of (5) become unfeasible as a whole. The first rows having an MPP voltage lower than $V_{inv_{min}}$ and higher than $V_{inv_{max}}$ are deleted. In this way, for the pilot example, if $V_{inv_{min}} = 60V$ and $V_{inv_{max}} = 130V$, the first three and the last three rows must be neglected and the power candidates are $241.0W$, $192.79W$, $239.68W$ and $199.74W$.

Finally, a set of power candidates corresponding to a minimum set of modules which are able to deliver a minimum value of the current are obtained. In order to find the real optimum, the P-V curve for each one of those candidates must be calculated. This detailed evaluation can be performed by an exact method, e.g. the one reported in [16], or by means of fast estimation algorithms like the ones reported in [12] and [11]. It is worth noting that the procedure proposed in this paper is able to reduce, significantly, the number of these time-consuming evaluations in comparison with an exhaustive search. For instance, in the proposed pilot example it is needed to test the single combination obtained by putting the three panels in series. Instead, an exhaustive search aimed at detecting the best MPP should have to test all the seven possible connections of the three panels into the string.

The pilot example has given as final best configuration that one involving all the three panels, which might seem almost obvious. The fact that such a conclusion is not always so evident is confirmed by the following second example involving again three PV panels, subjected to a rectangular irradiance profile, and exhibiting the I_{mpp} and V_{mpp} values presented in table II. The power matrix for this example is presented in (6), where the absolute maximum $395.0W$ is located at the coordinates (6,2): it means that six modules having a current higher than $3.5A$ are required. From the data set in table II it is recognized that such a condition is fulfilled by putting only panels #1 and #2 in series connection, this because the third panel would have affected the P-V curve only at voltages higher than the one at which the absolute MPP appears. The other power candidate in the range $395.0W - 23\% = [304.15, 395.0]W$ is $329.1W$. However, that candidate is neglected because it requires to work at the same current but at lower voltage than the previous one. Therefore, the absolute maximum $395.0W$ is the only candidate to be kept into consideration.

Table II
DATA SET OF PV PANELS IN THE SECOND EXAMPLE

Panels	V_{mpp_m} [V]	I_{mpp_m} [A]	MPP_m [W]	G $[W/m^2]$
P1	[19.5, 19.5, 19.5]	[4.5, 4.5, 4.5]	[87.8, 87.8, 87.8]	[900, 900, 900]
P2	[19.3, 19.3, 19.3]	[3.5, 3.5, 3.5]	[67.6, 67.6, 67.6]	[700, 700, 700]
P3	[17.5, 17.5, 17.5]	[0.5, 0.5, 0.5]	[8.8, 8.8, 8.8]	[100, 100, 100]

$$\begin{array}{c} \frac{I\Rightarrow}{V\Downarrow} \\ 18.8 \\ 37.5 \\ 56.3 \\ 75.0 \\ 93.8 \\ 112.5 \\ 131.3 \\ 150.1 \\ 168.8 \end{array} \begin{array}{c} |0.5 \\ \left(\begin{array}{c} 9.2 \\ 18.4 \\ 27.6 \\ 36.8 \\ 46.0 \\ 55.2 \\ 64.4 \\ 73.6 \\ 82.8 \end{array}\right. \end{array} \begin{array}{c} 3.5 \\ \begin{array}{c} 65.8 \\ 131.7 \\ 197.5 \\ 263.3 \\ \mathbf{329.1} \\ \underline{\mathbf{395.0}} \\ 0 \\ 0 \\ 0 \end{array} \end{array} \begin{array}{c} 4.5| \\ \left.\begin{array}{c} 84.9 \\ 169.7 \\ 254.6 \\ 0 \\ 0 \\ 0 \\ 0 \\ 0 \\ 0 \end{array}\right) \end{array} \tag{6}$$

In the following subsection the processing of this optimization algorithm is generalized.

V. DETAILED STEPS OF THE OPTIMIZATION ALGORITHM

In the previous sections the optimization algorithm oriented to the PV generator reconfiguration has been explained by means of a pilot example including three PV panels only. In this section the steps of the algorithm are generalized by referring to any string of panels having a number of modules, which is assumed to be the same for every panel. In the following the detailed steps of the optimization algorithm are listed:

1) Determine the coordinates (I_{mpp}, V_{mpp}) of the $(N_p \cdot M)$ total available modules by means of the procedure given in [10], [11] (refer to table I for the pilot example).
2) Build the vector of the MPP current candidates I_{mpp_k} by using the approximation given in (1) and including the number of multiplicities for all the elements of the vector (refer to (2) for the pilot example).
3) Build the vector of the MPP voltage candidates V_{mpp_k} (refer to (3) for the pilot example).
4) Determine the maximum voltage, thus the number of modules Qm_k, at which each I_{mpp_k} value can occur (refer to (4) for the pilot example).
5) Determine the power matrix by multiplying every V_{mpp_k} by every I_{mpp_k}. For each column, starting from the top, keep a number of power values equal to the number of modules able to provide that current, and put the remaining power values to zero (refer to (5) for the pilot example).
6) Cut off from the matrix the rows having a voltage value lower than the minimum MPPT inverter voltage and higher than the maximum MPPT inverter voltage.
7) Detect the MPP candidates: the maximum power value in the matrix and all the other power values in the range of -23% of it.
8) From the power matrix, the coordinates (row,column) of each MPP candidate determine the V_{mpp} candidate (row) and I_{mpp} candidate (column).
9) Access the database of the available PV modules and build up the corresponding PV string according to the following steps (refer to the flow chart in figure 6):
   a) Collect the modules ensuring at least a current equal to I_{mpp} candidate.
   b) Take, from the subset obtained in the previous step, a number of modules ensuring the I_{mpp} candidate.
   c) Build the string by collecting in series connection the panel owning the modules chosen at the previous step.
10) For each MPP candidate, calculate the P-V curve of the corresponding string determined at the previous step.
11) Select the configuration providing the absolute maximum power.

VI. EXTENSION OF THE OPTIMIZATION ALGORITHM TO ARRAYS

In the previous sections the proposed optimization algorithm was focused on PV strings. Its extension to PV arrays, which are the parallel connection of a number of strings, is proposed in this section. Also in this case a pilot example is used for a detailed explanation of the method. The differences with respect to the string-oriented approach are described, without any repetition of some concepts already examined in the simpler string case. The pilot example refers to four panels which have to be connected in two strings so that the whole array provides the maximum absolute power. In this example the mismatching conditions presented in table III are used. Also in this case the methods [10],[11] provides the data set presented in table III. Each one of the four panels ($N_p = 4$) is made of three PV modules, thus $M = 3$. Although the pilot example refers to two strings only, the extension of the method to any number of parallel connected strings is almost immediate. In the following, the same algorithm steps already presented for a single string are extended to the case of the array.

A. Array MPP current candidates

According to (1), also the MPP current candidates of an array appear at values that are close to the MPP current of its

Table III
DATA SET OF PV PANELS IN THE PILOT EXAMPLE OF AN ARRAY

Panels	V_{mpp_m} [V]	I_{mpp_m} [A]	MPP_m [W]	G $[W/m^2]$
P1	[19.5, 19.5, 19.5]	[4.5, 4.5, 4.5]	[87.8, 87.8, 87.8]	[900, 900, 900]
P2	[18.5, 18.5, 18.5]	[1.5, 1.5, 1.5]	[27.8, 27.8, 27.8]	[300, 300, 300]
P3	[19.4, 19.4, 17.6]	[4.0, 4.0, 1.6]	[77.6, 77.6, 28.2]	[800, 800, 300]
P4	[19.2, 18.5, 18.5]	[3.0, 1.5, 1.5]	[57.6, 27.8, 27.8]	[600, 300, 300]

strings. Figure 7 shows an example of two possible I-V curves corresponding to two strings forming an array and including the panels given in table III. The black curve is the I-V curve of the array, while the red and blue ones are the I-V curves of the strings. The red curve relates to the series connection of the panels P1 and P2, while the blue line refers to the series connection of panels P3 and P4. The MPPs of those curves are highlighted by square green markers. The gray square markers, instead, are the points, on each string, at the same voltage of the MPPs of the array. Figure 7 puts into evidence that the

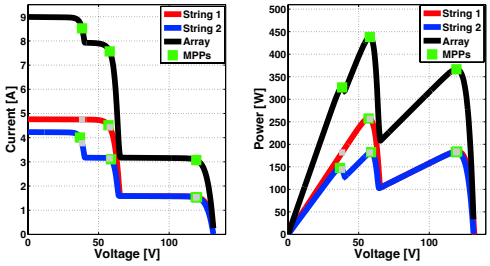

Figure 7. Relationship between the MPPs of an array and the MPPs of its strings

currents at which the green and the gray squares appear in every string are very close each other. This behavior holds in general. As a consequence, at any array MPP current its strings operate at some of their own MPP currents. Thus the MPP current candidates are all the possible combinations of the string MPP currents. The aspects discussed previously about the single string and concerning the multiplicity of candidates and the I_{mpp} clustering in a range of 5% are applied to arrays by a simple extension.

By referring to the pilot example, the strings and array MPP current candidates are given in (7) and (8), respectively.

$$I_{mpp_k} = [1.5_{(6)}, 3.0_{(1)}, 4.0_{(2)}, 4.5_{(3)}] \pm 5\% \tag{7}$$

$$I_{mpp_n} = [\{1.5_{(6)}, 3.0_{(1)}\}, \{1.5_{(6)}, 4.0_{(2)}\}, \{1.5_{(6)}, 4.5_{(3)}\}, \{3.0_{(1)}, 4.0_{(2)}\}, \{3.0_{(1)}, 4.5_{(3)}\}, \{4.0_{(2)}, 4.5_{(3)}\}, \{1.5_{(6)}, 1.5_{(6)}\}, \{3.0_{(1)}, 3.0_{(1)}\}, \{4.0_{(2)}, 4.0_{(2)}\}, \{4.5_{(3)}, 4.5_{(3)}\}] \pm 5\% \tag{8}$$

The length of the vector (8), which refers to the whole array, is $N_{I_{mpp}} = 10$.

B. Array MPP voltage candidates

As a consequence of the fact that the array and the strings MPP current candidates are almost similar, it is possible to obtain the MPP voltage candidates of the whole array by applying the same procedure previously discussed by referring to a string. For the pilot example, being the mean V_{mpp} value equal to 19.15 V, the array MPP voltage candidates are given in (9).

$$V_{mpp_n} = [19.15, 38.30, 57.45, 76.60, 95.75, 114.90] \pm 18\% \tag{9}$$

C. Array MPP candidates

By referring to the pilot example of table III, the modules that are able to work at the MPP current candidates have been named as M1 to M12 in table IV. In the same table, also the association between such modules and the panels they belong to is evidenced. It is worth noting that the module M1 is able to provide power when it is connected in a string working at any of the MPP current candidates. Instead, the module M12 must be connected into a string working at MPP current of $1.5A$. The MPP current candidates for the two strings adopted in the pilot example have been provided by (8). It is worth noting that, for the couple of MPP current candidates $I_{mpp_1} = \{1.5_{(6)}, 3.0_{(1)}\}$, table IV reveals that the modules M1 to M12 are able to work at $1.5A$, and the modules M1,M2,M3,M7,M8 and M10 are able to work at $3.0A$. For all the couples of MPP current candidates, the set of modules that are candidates at a high current value also includes the set of modules at a low current. However, the two strings cannot use the same modules candidates at the same time.

Table IV
MODULES OF THE PILOT EXAMPLE ABLE TO WORK AT MPP CURRENT CANDIDATES I_{mpp}

	P1			P2			P3			P4		
I_{mpp} [A]	M1	M2	M3	M4	M5	M6	M7	M8	M9	M10	M11	M12
1.5	⋆	⋆	⋆	⋆	⋆	⋆	⋆	⋆	⋆	⋆	⋆	⋆
3.0	⋆	⋆	⋆				⋆	⋆		⋆		
4.0	⋆	⋆	⋆				⋆	⋆				
4.5	⋆	⋆	⋆									

In (10), the amount of module candidates for each MPP current candidates of (8) have been calculated.

$$Qm_n^{'} = [\{12, 6\}, \{12, 5\}, \{12, 3\}, \{6, 5\}, \{6, 3\}, \{5, 3\}, \{12, 12\}, \{6, 6\}, \{5, 5\}, \{3, 3\}] \tag{10}$$

In order to obtain the real amount of module candidates able to work in the two strings separately, the amount of module candidates able to work at the lower current $I_{lower}(Qm_n^{'})$ is divided by the number of string in parallel (divided by two for the example under test). For example, the element Qm_4 provides that the amount of modules candidates for working at the lower current, $I_{lower}(Qm_4^{'}) = 3.0A$, is six, while the amount of modules candidates for working at the higher current, $I_{higher}(Qm_4^{'}) = 4.0A$, is five. Thus, these two strings, working at the same time, have three modules able to work at $3.0A$, and five modules able to work at $4.0A$. Because it has been assumed that the two strings connected in parallel must have the same number of panels, the final amount of modules to be selected for each string is the lower value among the

two amounts of candidates. In (11), this procedure to obtain the real amount of module candidates has been formalized. By using (11) in (10), the final vector of minimum number of active modules at MPP current candidates Qm_n is given in (12).

$$Qm_n = min\left\{\frac{I_{lower}(Qm_n^{'})}{2}, I_{higher}(Qm_n^{'})\right\} \tag{11}$$

$$Qm_n = [\{6,6\},\{5,5\},\{3,3\},\{3,3\},\{3,3\},\{2,2\},\{6,6\},\{3,3\},\{2,2\},\{1,1\}] \tag{12}$$

As a last step, similarly to the case of the string previously shown, the matrix representation (13) of the MPP candidates is calculated. The absolute maximum power is 527.67 W, which is obtained by using five modules per string that are able to work at $1.5A$ and $4.0A$, respectively. By inspecting the features of each module in table III, it results that the first string includes panels P1 and P3, while the second string includes panels P2 and P4. As for the case of the single string, other possible MPP candidates must be evaluated up to the power $527.67W - 23\% = [406.31]W$. For example, the candidate $515.97W$ requires six modules in each string able to work at $1.5A$ and $3.0A$. The data set given in table III reveals that there are some modules fulfilling such requirements, but there is not a configuration of panels providing those conditions in the two strings separately. In the same way, there is not a solution for the candidate $431.93W$. The other two candidates, $429.98W$ and $422.64W$, generate the same solution of the global candidate $527.67W$.

$\frac{I_{mpp}}{V_{mpp}}$	$\lvert 1.5,3.0$	$1.5,4.0$	$1.5,4.5$	$3.0,4.0$	$3.0,4.5$	$4.0,4.5$	$1.5,1.5$	$3.0,3.0$	$4.0,4.0$	$4.5,4.5\rvert$
19.15	86.00	105.53	115.30	134.21	143.98	163.52	57.32	114.67	153.75	173.28
38.30	172.00	211.07	230.61	268.42	287.95	327.03	114.64	229.34	307.50	0
57.45	258.00	316.60	345.91	402.62	**431.93**	0	171.97	344.01	0	0
76.60	343.98	**422.14**	0	0	0	0	229.29	0	0	0
95.75	**429.98**	**527.67**	0	0	0	0	286.61	0	0	0
114.90	**515.97**	0	0	0	0	0	343.93	0	0	0

(13)

VII. Evaluation of the Optimization Algorithm with a Large PV Array

In this section the results of the application of the proposed algorithm to a large array of two strings of panels connected in parallel is presented. With respect to the pilot examples proposed in the previous part of the manuscript, which were aimed at describing the procedure, the test proposed in this section looks more realistic. Twelve PV panels ($N_p = 12$), each one formed by three modules ($M = 3$), are considered. The panels are physically organized as it is shown in figure 8. Shadows affect panels P1 and P2 as well as P4 and P5. The irradiance values assigned to each module are given in table V.

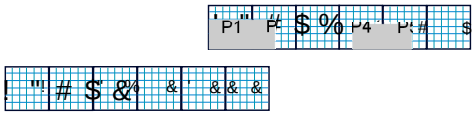

Figure 8. The shadowing pattern for the large PV array example

It is assumed that the inverter is able to perform its MPPT function in the range defined by $V_{inv_{min}} = 200V$ and $V_{inv_{max}} = 350V$. By accounting for the fact that the twelve panels can be organized in two different strings, formula (14) reveals that the exhaustive algorithm requires to test $C = 26103$ different combinations.

Table V
Data set of PV panels presented in figure 8

Panels	V_{mpp_m} [V]	I_{mpp_m} [A]	MPP_m [W]	G $[W/m^2]$
P1	[19.5, 17.3, 17.3]	[5.0, 0.5, 0.5]	[19.5, 8.7, 8.7]	[1000, 100, 100]
P2	[19.6 18.9 18.9]	[5.0 2.6 2.6]	[98, 49.1, 49.1]	[1000, 500, 500]
P3, P6 to P12	[19.6, 19.6, 19.6]	[5.0, 5.0, 5.0]	[98, 98, 98]	[1000, 1000, 1000]
P4, P5	[19.6, 19.2, 17.6]	[5.0, 2.6, 1.6]	[98, 49.9, 28.2]	[1000, 500, 300]

$$C = \frac{1}{2}\sum_{s=4,5,6}\frac{(N_P)!}{(2s)!\cdot(N_P-2s)!}\cdot\frac{(2s)!}{(s)!\cdot(s)!} \tag{14}$$

The best configuration obtained at the end of the exhaustive search is given in table VI and it is the same achieved by the optimization algorithm proposed in this paper. In Figure 10, the blue line is obtained by the exhaustive algorithm using the single diode model (SDM) and the method developed in [16]. The maximum power point MPP is highlighted in green square marker, and its value is 2737.3 W at 272.4 V.

Table VI
PV panels selected for the two strings $\mathbf{S_{t1}}$,$\mathbf{S_{t2}}$

$\mathbf{S_{t1}}$	P1	P2	P3	P6	P7	P8
$\mathbf{S_{t2}}$	P4	P5	P9	P10	P11	P12

The MPP current and voltage candidates used by the algorithm proposed in this paper are (15) and (16), respectively, where the subscript shows, as already done above, the multiplicity of I_{mpp}. Also, the vector of minimum number of active modules at MPP current candidates Qm_n is given in (17).

$$I_{mpp_n} = [\{0.5_{(2)},1.6_{(2)}\},\{0.5_{(2)},2.6_{(4)}\},\{0.5_{(2)},5.0_{(28)}\},\{1.6_{(2)},2.6_{(4)}\},\{1.6_{(2)},5.0_{(28)}\},\{2.6_{(4)},5.0_{(28)}\},\{0.5_{(2)},0.5_{(2)}\},\{1.6_{(2)},1.6_{(2)}\},\{2.6_{(4)},2.6_{(4)}\},\{5.0_{(28)},5.0_{(28)}\}] \pm 5\% \tag{15}$$

$$V_{mpp_n} = [19.6, 39.2, 58.8, 78.4, 98.0, 117.6, 137.1, 156.7, 176.3, 195.9, 215.5, 235.1, 254.7, 274.3, 293.9, 313.5, 333.1, 352.7] \pm 18\% \tag{16}$$

$$Qm_n = [\{18,18\},\{18,18\},\{18,18\},\{17,17\},\{17,17\},\{16,16\},\{18,18\},\{17,17\},\{16,16\},\{14,14\}] \tag{17}$$

The power matrix is obtained by means of the same procedure already explained for the previous examples, and it is shown in (18). That matrix provides the MPP candidate with a power value that is equal to $2745.1W$ at $274.3V$. It appears at the fourteenth row and at the tenth column of the matrix itself. This position indicates that fourteen modules that are able to work at $5.0A$ are needed for each string. The steps of the proposed algorithm are the same ones presented in Section V. Each MPP current candidate is the couple of data provided by (15), so that the ninth step of the optimization algorithm is changed according to what is reported in the flow chart shown in figure 9. First, the required number of modules, which are able to work at the higher MPP current candidate, is collected. All the combinations of the twelve

panels are arranged in a look up table: it contains 495, 792 and 924 different configurations that are obtained when six, five and four panels, respectively, are collected to form a string. Those amount of panels per string allow to fulfill the input voltage range defined by the inverter. The right side of figure 9 refers to the case of six panels per string: the first combination collecting fourteen modules that are able to work at $5.0A$ is $\mathbf{S_{t1}} = [P1, P2, P3, P6, P7, P8]$. This solution is assigned to the string $\mathbf{S_{t1}}$. In order to achieve the solution for the second string, a further run of the searching algorithm, in which the MPP current candidate is $5.0A$ again, is needed. In this case only one solution results, which is $\mathbf{S_{t2}} = [P4, P5, P9, P10, P11, P12]$. This array configuration coincides with the one achieved by the exhaustive algorithm, as it is shown in table VI.

$\frac{I \Rightarrow}{V \Downarrow}$	$\|0.5, 1.6$	$0.5, 2.6$	$0.5, 5.0$	$1.6, 2.6$	$1.6, 5.0$	$2.6, 5.0$	$0.5, 0.5$	$1.6, 1.6$	$2.6, 2.6$	$5.0, 5.0\|$
19.6	40.2	59.7	107.9	80.3	128.4	148.0	19.6	60.8	99.8	196.1
39.2	80.4	119.5	215.7	160.6	256.9	295.9	39.3	121.6	199.7	392.2
58.8	120.6	179.2	323.6	240.9	385.3	443.9	58.9	182.3	299.5	588.2
78.4	160.8	239.0	431.4	321.2	513.7	591.9	78.5	243.1	399.4	784.3
98.0	201.0	298.7	539.3	401.6	642.2	739.8	98.2	303.9	499.2	980.4
117.6	241.3	358.4	647.2	481.9	770.6	887.8	117.8	364.7	599.1	1176.5
137.1	281.5	418.2	755.0	562.2	899.0	1035.7	137.4	425.5	698.9	1372.6
156.7	321.7	477.9	862.9	642.5	1027.4	1183.7	157.1	486.2	798.7	1568.7
176.3	361.9	537.7	970.7	722.8	1155.9	1331.7	176.7	547.0	898.6	1764.7
195.9	402.1	597.4	1078.6	803.1	1284.3	1479.6	196.4	607.8	998.4	1960.8
215.5	442.3	657.1	1186.4	883.4	1412.7	1627.6	216.0	668.6	1098.3	**2156.9**
235.1	482.5	716.9	1294.3	963.7	1541.2	1775.6	235.6	729.4	1198.1	**2353.0**
254.7	522.7	776.6	1402.2	1044.1	1669.6	1923.5	255.3	790.1	1298.0	**2549.1**
274.3	562.9	836.4	1510.0	1124.4	1798.0	2071.5	274.9	850.9	1397.8	**2745.1**
293.9	603.1	896.1	1617.9	1204.7	1926.5	**2219.4**	294.5	911.7	1497.7	0
313.5	643.3	955.8	1725.7	1285.0	2054.9	**2367.4**	314.2	972.5	1597.5	0
333.1	683.5	1015.6	1833.6	1365.3	**2183.3**	0	333.8	1033.3	0	0
352.7	723.7	1075.3	1941.5	0	0	0	353.4	0	0	0

(18)

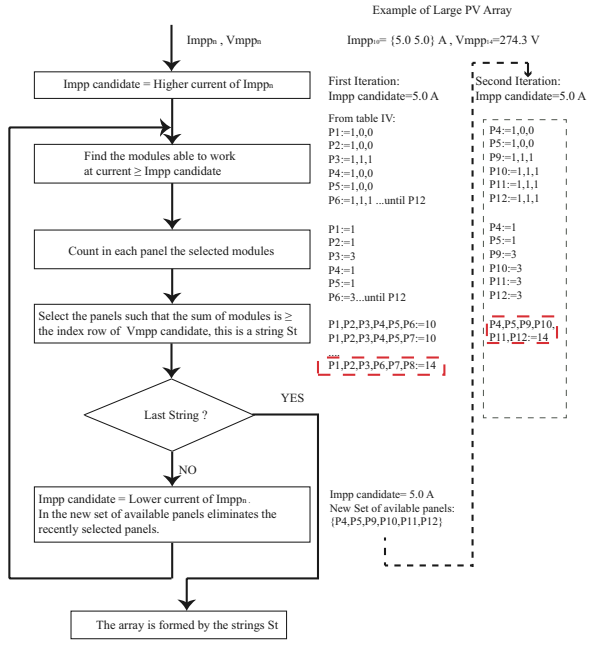

Figure 9. Flow Chart of the searching algorithm of configurations for arrays

In addition, the two following configurations Cf_1 and Cf_2 fulfill the same condition: $\mathrm{Cf}_1 = \{\mathbf{S_{t1}} = [P1, P5, P3, P6, P7, P8], \mathbf{S_{t2}} = [P2, P4, P9, P10, P11, P12]\}$, and $\mathrm{Cf}_2 = \{\mathbf{S_{t1}} = [P1, P4, P3, P6, P7, P8], \mathbf{S_{t2}} = [P2, P5, P9, P10, P11, P12]\}$. In figure 10, the P-V curves corresponding to Cf_1 and Cf_2 in red and black color, respectively, are shown. Configurations Cf_1 and Cf_2 provide the same P-V curve with the same MPP value, which is $2745.1W$. This is due to the fact that there is several modules exhibiting the same irradiance profile, thus different combinations produce the same curve in a large range of the voltage, which include the MPP. In figure 10 with cyan and red square markers the MPP values of these configurations obtained from the power matrix at $2745.1W$ are put into evidence. By using the fast estimation method [11] it results a power value equal to $2736.8W$. The power errors of these MPP values, compared with the MPP provided by the exhaustive algorithm ($2737.3W$), are 0.28% and 0.02%, respectively.

By keeping into account the MPP power interval, the other MPP candidates in the range given by a power derating $2745.1W - 23\%$, thus in the interval $[2137.0, 2745.1]W$, have to be evaluated as well. The MPP candidate $2549.1W$ provides the same configuration candidates Cf_1 and Cf_2, while the candidates $2367.4W$ and $2219.4W$ provide a new candidate $\mathrm{Cf}_3 = \{\mathbf{S_{t1}} = [P1, P3, P6, P7, P8, P9], \mathbf{S_{t2}} = [P2, P4, P5, P10, P11, P12]\}$. The P-V curve of Cf_3 is shown in magenta color in figure 10, where its MPP power ($2403W$) is observed. In the same way, the candidates $2353W$ and $2156.9W$ provide the new configuration candidate $\mathrm{Cf}_4 = \{\mathbf{S_{t1}} = [P3, P6, P7, P8], \mathbf{S_{t2}} = [P9, P10, P11, P12]\}$. The P-V curve corresponding to Cf_4 is shown in grey color in figure 10: its MPP power value is equal to $2365W$, which is very close to the guess one provided by the power matrix. Those other candidates Cf_3 and Cf_4 provide array power levels lower than $2745.1W$, which is the power provided by the first MPP candidate. Finally, there is not a solution for the candidate $2183.3W$.

The simulations were performed using a AMD Phenom(tm) 9650 Quad-Core 2.31 GHz processor and 2.0 GB of RAM memory. The calculation time used by the proposed estimation method was 165.2 ms, which is significantly lower than the 57 h. 57 m. 55 s needed by the exhaustive search algorithm.

In conclusion, the proposed optimization method provides a solution with an error lower than 1%, but spending an execution time of six orders of magnitude lower than the one required by the exhaustive search. The proposed optimization algorithm confirms to be useful to search, in a reasonable time, the global solution of the reconfiguration of panels, which is a complex combinatorial optimization problem.

VIII. Conclusion

In this paper an optimization algorithm for reconfiguring PV panels has been proposed. The algorithm provides an optimized solution taking into account the input voltage constraints of the inverter. In the first step of the algorithm, the feasible voltage and current intervals where the MPP falls are determined. These intervals are organized in a matrix power where the searching of the solution is started from the global optimum power. The size of the feasible intervals includes voltage and current values of PV panels exhibiting

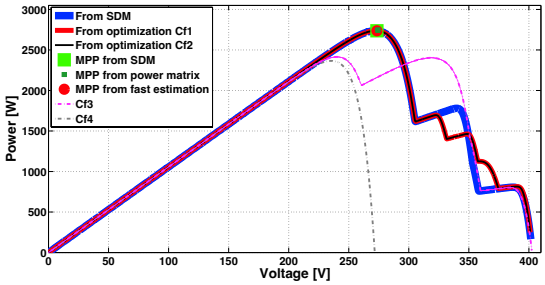

Figure 10. P-V curves of the array formed by the different configuration candidates

the poor cases of fill factor. Thus, the set of MPP candidates includes all the feasible practical solutions. If there are several configurations providing the same MPP candidate, a fast estimation method for approximating the MPP is used. The proposed optimization algorithm has been validated by comparison with an exhaustive algorithm, where a PV field of twelve PV panels subjected to practical shadow profile has been used. The solution provided by the optimization algorithm is the same from exhaustive algorithm, but the calculation time was reduced in six orders of magnitude, thus the proposed optimization algorithm is useful for on-line PV applications.

ACKNOWLEDGMENT

This work was supported by Universidad del Valle (Colombia), Colciencias (Fondo nacional de financiamiento para ciencia, la tecnología y la innovación Francisco José de Caldas, Colombia) under the project MicroRENIZ-25439 (Code 1118-669-46197) and Scholarship 528-2011, University of Salerno and Universidad Nacional de Colombia.

REFERENCES

[1] E. Koutroulis and F. Blaabjerg, "A new technique for tracking the global maximum power point of pv arrays operating under partial-shading conditions," *IEEE Journal of Photovoltaics*, vol. 2, no. 2, pp. 184–190, 2012.

[2] G. Spagnuolo, G. Petrone, B. Lehman, C. Ramos-Paja, Y. Zhao, and M. Orozco-Gutierrez, "Control of photovoltaic arrays: Dynamical reconfiguration for fighting mismatched conditions and meeting load requests," *IEEE Industrial Electronics Magazine*, vol. 9, pp. 62–76, 2015.

[3] D. LaManna, V. LiVigni, E. RivaSanseverino, V. D. Dio, and P. Romano, "Reconfigurable electrical interconnection strategies for photovoltaic arrays: A review," *Renewable and Sustainable Energy Reviews*, vol. 33, p. 412ñ426, 2014.

[4] J. Storey, P. R. Wilson, and D. Bagnall, "The optimized-string dynamic photovoltaic array," *IEEE Transaction on Power Electronics*, vol. 29, no. 4, p. 1768ñ1776, 2014.

[5] E. L. Lawler, *Combinatorial Optimization: Networks and Matroids*. Holt, Rinehart and Winston, 1976.

[6] G. Velasco-Quesada, F. Guinjoan-Gispert, R. Pique-Lopez, M. Roman-Lumbreras, and A. Conesa-Roca, "Electrical pv array reconfiguration strategy for energy extraction improvement in grid-connected pv systems," *IEEE Transaction on Industrial Electronics*, vol. 56, no. 11, p. 4319ñ4331, 2009.

[7] J. P. Storey, P. R. Wilson, and D. Bagnall, "Improved optimization strategy for irradiance equalization in dynamic photovoltaic arrays," *IEEE Transaction on Industrial Electronics*, vol. 28, no. 6, p. 2946ñ2956, 2013.

[8] M. Z. S. El-Dein, M. Kazerani, and M. M. A. Salama, "An optimal total cross tied interconnection for reducing mismatch losses in photovoltaic arrays," *IEEE Transaction on Sustainable Energy*, vol. 4, no. 1, p. 1768ñ1776, 2013.

[9] P. Carotenuto, A. D. Cioppa, A. Marcelli, and G. Spagnuolo, "An evolutionary approach to the dynamical reconfiguration of photovoltaic fields," *Neurocomputing*, vol. 170, p. 393ñ405, 2015.

[10] P. Carotenuto, P. Manganiello, G. Petrone, and G. Spagnuolo, "Online recording a pv module fingerprint," *IEEE Journal of Photovoltaics*, vol. 4, no. 2, pp. 659–668, March 2014.

[11] M. Orozco-Gutierrez, J. Ramirez-Scarpetta, G. Spagnuolo, G. Petrone, and C. Ramos-Paja, "Fast estimation of mpps in mismatched pv arrays based on lossless model," *International Conference on Clean Electrical Power (ICCEP)*, pp. 435–440, 2015.

[12] M. Orozco-Gutierrez, G. Petrone, J. Ramirez-Scarpetta, G. Spagnuolo, and C. Ramos-Paja, "A method for the fast estimation of the maximum power points in mismatched pv strings," *Electric Power Systems Research*, vol. 121, pp. 115–125, 2015.

[13] J.-C. Wang, Y.-L. Su, J.-C. Shieh, and J.-A. Jiang, "High-accuracy maximum power point estimation for photovoltaic arrays," *Solar Energy Materials and Solar Cells*, vol. 95, p. 843ñ851, 2011.

[14] S. Moballegh and J. Jiang, "Modeling, prediction, and experimental validations of power peaks of pv arrays under partial shading conditions," *IEEE Transactions on Sustainable Energy*, vol. 5, pp. 293–300, 2014.

[15] J. Maa, K. Man, T. Ting, N. Zhang, S.-U. Guan, and P. Wonga, "Dem: Direct estimation method for photovoltaic maximum power point tracking," *Procedia Computer Science*, vol. 17, p. 537ñ544, 2013.

[16] M. Orozco-Gutierrez, J. Ramirez-Scarpetta, G. Spagnuolo, and C. Ramos-Paja, "A technique for mismatched pv array simulation," *Renewable Energy*, vol. 55, no. 0, pp. 417 – 427, 2013.